Restoration of Guyton Diagram for Regulation of the Circulation as a Basis for Quantitative Physiological Model Development

J. KOFRÁNEK[1], J. RUSZ[1,2]
[1]Charles University in Prague, 1st Faculty of Medicine, Department of Pathophysiology, Laboratory of Biocybernetics, Czech Republic
[2]Czech Technical University in Prague, Faculty of Electrical Engineering, Department of Circuit Theory, Czech Republic

Corresponding author
Jan Rusz
Department of Circuit Theory
Faculty of Electrical Engineering
Czech Technical University
Technicka 2
166 27 Prague 6
Czech Republic
EU

e-mail: ruszjan@fel.cvut.cz

Short title
Restoration of Guyton Diagram

Summary

We present the current state of complex circulatory dynamics model development based on Guyton's famous diagram. The aim is to provide an open-source model that will allow the simulation of a number of pathological conditions on a virtual patient including cardiac, respiratory, and kidney failure. The model will also simulate the therapeutic influence of various drugs, infusions of electrolytes, blood transfusion, etc. As a current result of implementation, we describe a core model of human physiology targeting the systemic circulation, arterial pressure and body fluid regulation, including short- and long-term regulations. The model can be used for educational purposes and general reflection on physiological regulation in pathogenesis of various diseases.

Key words

Body fluid homeostasis; Blood pressure regulation; Physiological modelling; Guyton diagram

Introduction

The landmark achievement closely associated with integrative physiology development was the circulatory dynamics model published by prof. A. C. Guyton and his collaborators in 1972 (Guyton *et al.* 1972). Subsequently, its more detailed description was published in the monograph one year later (Guyton *et al.* 1973). This model represents the first large-scale mathematical description of the body's interconnected physiological subsystems. The model was described by a sophisticated graphic diagram with various computing blocks symbolizing quantitative physiological feedback connections. The diagram was published as a picture and the actual realization of the model was implemented in the *FORTRAN* language.

Although the FORTRAN implementation worked correctly, the diagram contains a number of errors that cause wrong model behaviour. Moreover, FORTRAN implementation is not in correspondence with this famous graphic diagram, it is almost unavailable nowadays, and contains several programming and computation-related features that require special treatment (Thomas *et al.* 2008). Despite the fact that the model was published over 30 years ago, it is currently used as a base for a number of research studies in the field of physiology (Montani and Van Vliet 2009, Osborn *et al.* 2009) and physiological modelling (Bassingthwaighte 2000, Hunter *et al.* 2002, Thomas *et al.* 2008, Bassingthwaighte 2009), including research on the physiological consequences of weightlessness in manned space flight (White *et al.* 1991, White *et al.* 2003), or in a new approach to automation in medicine (Nguyen *et al.* 2008). In addition, the diagram is still reprinted with the original errors (Hall 2004, Bruce and Montani 2005). The overall revision of the diagram requires exhaustive search for errors and sophisticated analyses of physiological regulations system.

Here, we present a prototype of a core model of human physiology based on the original Guyton diagram targeting the short- and long-term regulation of blood pressure, body fluids and homeostasis of the major solutes. This model also includes the hormonal (antidiuretic

hormone, aldosterone and angiotensine) and nervous regulators (autonomic control), and the main regulatory sensors (baro- and chemo-receptors). Our complex circulatory dynamics model corresponds to the same graphic notation of the original Guyton diagram and keeps adheres to its basic physiological principles. While new models are continuously being developed (Srinivasan *et al.* 1996, Abram *et al.* 2007, Hester *et al.* 2008), our model finally brings a fully functional modification to the original Guyton diagram, which is more suitable for a better and deeper understanding of the importance of physiological regulations and their use in development of many pathophysiological conditions by using simulation experiments.

The resulting model can be used as a baseline for the quantitative physiological model development designated for physicians' e-learning and acute care medicine simulators. Another use of the model is as an effective learning aid for physiological regulation systems education, connected with biomedical engineering specialization. The model is provided as an open-source and it is downloadable at <http://physiome.cz/guyton/>.

Methods

Mathematical model of global physiological regulation of blood pressure

The model consists of 18 modules containing approximately 160 variables and including 36 state variables (see Table 1 for more details). Each module represents an interconnected physiological subsystem (kidney, tissue fluid, electrolytes, autonomous nervous regulation and hormonal control including antidiuretic hormone, angiotensine and aldosterone). The model is constructed around a 'central' *circulatory dynamics* module in interaction with 17 'peripheral' modules corresponding to physiological functions (see figure 1) and complete model targeting the systemic circulation, arterial pressure and body fluid regulation, including short- and long-term regulations. A graphic presentation of the model allows a display of the connectivity among all physiological relationships. In essence, the model contains a total of

approximately 500 numerical entities (model variables, parameters and constants). Members of the original Guyton laboratory have been continuously developing a more sophisticated version of the model, which is used for teaching (Abram *et al.* 2007). Although it includes about 4000 variables, this more elaborate model is less suited for our purposes then 1972 Guyton et al. model, because of its incomplete description and physiological relationships formulation.

Physiological regulations system analyses

The original model represented as a sophisticated graphic diagram contains a number of errors which imply entirely incorrect physiological model behaviour. The correction of these errors demanded complicated physiological regulations system analyses. These include exhaustive revision of the complete model and its behaviour validation using several simulation experiments. In this stage, the original FORTRAN code of the Guyton *et al.* model was also used to compare the obtained simulation results. It is of course the case that the original FORTRAN code runs correctly; the errors were only in the diagram.

Because it would be beyond the scope of this paper to discuss each error in the original Guyton diagram, as an example of the system analyses, we describe the five most significant errors which would have the greatest role in creating the unpredictable model behaviour (see figure 2). The other errors are mostly caused by replaced mathematical operations, wrong set of normalization and damping constants, and replaced signs that determine the positive or negative feedback.

The first error is the wrong flow direction marking of blood flow in the *circulatory dynamics* subsystem (see figure 2a). The rate of increase in systemic venous vascular blood volume (DVS) is the subtraction between all rates of inflows and rates of outflows. Blood flow from the systemic arterial system (QAO) means inflow and rate from veins into the right

atrium (QVO) means outflow. Rate change of the vascular system filling as the blood volume changes (VBD) is calculated as the difference between the summation of vascular blood compartments and blood volume overall capacity, meaning that VBD is found in the outflow rate too. Equation (1) gives DVS:

$$\text{Correct eq.: } DVS = QAO - VBD - QVO,$$
$$\text{Erroneous eq.: } DVS = QAO + VBD + QVO. \quad (1)$$

The second error is an algebraic loop in the *non-muscle oxygen delivery* subsystem (see figure 2b). There is a wrong feedback connection in venous oxygen saturation (OSV), which would cause a constant rise of OSV and the model would rapidly became unstable. Equation (2) gives the OSV from the blood flow in non-renal, non-muscle tissues (BFN), oxygen volume in aortic blood (OVA), rate of oxygen delivery to non-muscle cells (DOB) and hematocrit (HM),

$$\text{Correct eq.: } \frac{d(OSV)}{dt} = \left(\frac{BFN \times OVA - DOB}{BFN \times HM \times 5} - OSV \right) / Z7,$$
$$\text{Erroneous eq.: } \frac{d(OSV)}{dt} = \frac{BFN \times OVA - DOB}{BFN \times HM \times 5} - \frac{BFN \times OVA - DOB}{BFN \times HM \times 5 \times Z7}. \quad (2)$$

Errors 3 and 4 involve simple subsystem *red cells and viscosity*. The third one is caused by positive feedback in the volume of red blood cells (VRC) computation (see figure 2c). Equation (3) gives the VRC from the red cell mass production rate (RC1) and rate factor for red cells destruction (RCK) where the product between VRC and RCK gives the red cell mass destruction rate,

Correct eq.: $\frac{d(VRC)}{dt} = RC1 - VRC \times RCK,$

Erroneous eq.: $\frac{d(VRC)}{dt} = RC1 + VRC \times RCK.$ (3)

The fourth error is caused by a missing negative feedback in the portion of blood viscosity caused by red blood cells (VIE) computation (see figure 2d). VIE is computed from the output of integrator HM2 (HM after integration divided by the normalization parameter HKM). Without the negative feedback, HM2 would incessantly rise. Viscosity is proportionate to hematocrit and the integrator acts as a dampening element in the original Guyton *et al.* model. From experimental data it can be derived that dependence of blood viscosity on hematocrit is not linearly proportional (Guyton *et al.* 1973). In equation (4), we designed a negative feedback by adding HMK constant into the feedback and by changing the HKM normalization parameter, which caused stabilized behaviour of HM2,

Correct eq.: $\frac{d(HM2)}{dt} = HM - \frac{HM2}{HMK},$

Erroneous eq.: $\frac{d(HM2)}{dt} = HM.$ (4)

The fifth error is in the *antidiuretic hormone control* subsystem. The problem is in normalized antidiuretic hormone control computation (AHC) and normalized rate of antidiuretic hormone creation (AH $\times$ 0.3333) computation (see figure 2e), when both values have a value of 1 under normal conditions. The solution emerges from the classic compartment approach. The hormone inflows into the whole-body compartment at the rate F_1

and outflows at the rate F_O. Rate of its depletion is proportional to its concentration c, where $F_O = k \times c$, and concentration depends on overall quantity of hormone *M* and on capacity of distribution area *V*. Equation (5) gives the quantity of hormone *M* in whole-body compartment, which depends on balance between hormone inflow and outflow,

$$\frac{dM}{dt} = F_I - \frac{kM}{V}. \tag{5}$$

Provided that the capacity of distribution area *V* is constant, we will substitute the ratio *k/V* with constant k_1. Guyton calculated the concentration of hormone c_0 normalized as a ratio of current concentration *c* to its normal value $c_{norm} = c/c_0$. At invariable distribution area *V*, ratio of concentrations is the same as a ratio of current hormone overall quantity *M* to overall hormone quantity under normal conditions $M_{norm} = M/c_0$. When we formulate the rate of flow in a normalized way (as a ratio to normal rate), under normal conditions it holds that $F_I = 1$, $dM_{norm}/dt = 0$ and after substituting it into equation (5) we get the equation (6),

$$1 - k_1 M_{norm} = 0. \tag{6}$$

The relative concentration of hormone c_0 can be formulated as equation (7),

$$c_0 = \frac{M}{M_{norm}} = k_1 M, \tag{7}$$

and after final adjustments and inserting into a differential equation (7) we arrive at

Correct eq.: $\frac{dc_0}{dt} = (F_I - c_0)k_1,$ (8)

Erroneous eq.: $\frac{dc_0}{dt} = F_I - c_0 k_1.$ (9)

According to equation (8), the normalized concentration of hormone c_0 is subtracted from normalized inflow of hormone F_I. In the original Guyton diagram, the normalized concentration of aldosterone and angiotensine is calculated this way, which means that normalized rate of inflows is F_1 = AH $\times$ 0.3333 and normalized concentration of hormone is c_0 = AHC. As a result, AHC is represented by equation (9) instead of equation (8) in the original Guyton diagram. Equation (10) gives the final relation of AHC represented in model:

Correct eq.: $\frac{d(AHC)}{dt} = (AH \times 0.3333 - AHC) \times 0.14,$

Erroneous eq.: $\frac{d(AHC)}{dt} = AH \times 0.3333 - AHC \times 0.14.$ (10)

Model under SIMULINK

SIMULINK is a block-based language for describing dynamic systems, and also works as a modelling and simulation platform (we used version 7.5.0.342 - R2007b, integrated with MATLAB, The MathWorks, Nattick, MA, USA). It is an interactive and graphic environment dedicated to the multi-domain simulation of hybrid continuous/discrete systems. During simulations, model and block parameters can be modified, and signals can be easily accessed and monitored. In the model, numerical integration was performed using ‘ode13t’ (a

MATLAB library) with a variable step size (maximum step size, auto; relative tolerance, 10K3).

First, code operations and routines from the computer program were rendered into the SIMULINK graphical description, i.e. elementary blocks and subsystems were connected by appropriate signals and the graphic notation of the original Guyton diagram was kept as much as possible (Kofránek and Rusz 2007).

Second, subsystems were not treated as 'atomic subunits'. This causes SIMULINK's solver to treat each subsystem as a complete functioning model. Technically, the model works in continuous time and performs all physiological regulations as a complete unit (as the original graphic diagram was designed – the FORTRAN implementation of the model is characterized by a wide range of time scales in the different subsystems), which provides an advantage when designing control systems using principles of complex physiological regulation. All calculations were performed using only the original damping constants obtained from Guyton diagram.

Finally, to remove a lack of convergence due to oscillation and other run-time errors, the model has addressed the algebraic loops. Note that complex model behaviour depends also on correct communication between all subsystems. In this case, it was essential to normalize some of the experimental set and damping constants and supervise model behaviour. The complete model is available as open-source on <http://physiome.cz/guyton/>.

Model validation

In order to validate our corrected SIMULINK implementation of the Guyton diagram, we simulated four experiments described in the (Guyton *et al.* 1972) paper and compared the results with clinic data measurements in a series of six dogs, data adopted from (Chau *et al.* 1979), and the original Guyton *et al.* model implementation in the FORTRAN environment.

The first experiment is the simulation of hypertension in a salt-loaded, renal-deficient patient by decreasing the functional renal mass to ~ 30% of normal and increasing the salt intake to about five times normal on *day 0*. This is a very fundamental experiment revealing the importance of the kidneys in blood-pressure control and their influence in the development of essential hypertension (Langston *et al.* 1963, Douglas *et al.* 1964, Coleman and Guyton 1969, Cowley and Guyton 1975). The duration of the whole experiment is 12 days.

The second benchmark experiment represents sudden severe muscle exercise and takes place over a much shorter time scale than other experiments (5 min). The exercise activity was increased to sixty times the normal resting level by setting the exercise activity-ratio with respect to activity at rest after 30 second, corresponding to an approximately 15-fold increase in the whole-body metabolic rate (in this case, the time constant for the local vascular response to metabolic activity was reduced by 1/40).

The third benchmark experiment simulates the progress of nephrotic edema by increasing seven-fold the rate of plasma-protein loss on *day 1*. After seven days, the rate of plasma-protein loss is reduced to three-times above the norm. The duration of the whole experiment is 12 days.

The fourth benchmark experiment simulates the atrioventricular fistula by opening the fistula on *day 1* (the constant that represents fistula is set to 5%) and closing the fistula on *day 5*. The duration of the whole experiment is 9 days.

The goodness-of-fit of the model was also compared in terms of the chi-square (χ^2) test between observed simulation results and predicted clinical data.

Results

Figure 3 represents the results of the simulation of hypertension (1. experiment). The cardiac output rose at first to ~ 30% above normal but then was stabilized by the end of 12 days. The arterial pressure rises more slowly, requiring several days to reach high elevation. During the next days it remained at its new high level indefinitely, as long as the high salt intake was maintained. The simulation is quite sufficient to predict the available data with high statistical significances of χ^2 (11) = 1445; $p < 0.001$ for simulation of the arterial pressure, χ^2 (10) = 939; $p < 0.001$ for simulation of the heart rate, χ^2 (10) = 1388; $p < 0.001$ for simulation of the stroke volume, χ^2 (10) = 1189; $p < 0.001$ for simulation of the cardiac output, and χ^2 (10) = 1304; $p < 0.001$ for simulation of the total peripheral resistance.

Figure 4 presents the results of the muscle exercise simulation (2. benchmark experiment). At the onset of exercise, cardiac output and muscle blood flow increased considerably and within a second. Urinary output fell to its minimal level, while arterial pressure rose moderately. Muscle cell and venous PO_2 fell rapidly. Muscle metabolic activity showed an instantaneous increase but then decreased considerably because of the development of a metabolic deficit in the muscles. When exercise was stopped, muscle metabolic activity fell below normal, but cardiac output, muscle blood flow and arterial pressure remained elevated for a while as the person was repaying their oxygen dept.

Figure 5 illustrates the results of the nephrosis simulation (3. benchmark experiment). The principal effect of nephrosis consists of urine protein excretion that may or may not be associated with any significant changes in other renal functions. A deficit of the total plasma protein reduces the oncotic pressure, resulting in a fluid redistribution from the blood to the interstitial compartment and an increase of the (mostly free-) interstitial-fluid volume. Another effect is mild decreases of cardiac output and arterial pressure. The initial hypoproteinemia only slightly decreased both arterial pressure and cardiac output but induced

a notable restriction of the urinary output. Thus, the fluid was being retained in the organism causing the interstitial swelling, although the volume of the free interstitial fluid remained relatively unchanged until the interstitial-fluid pressure stayed negative. After it reached positive values, an apparent edema occurred with a sharp drop in the arterial pressure. When the rate of renal loss of protein was increased to the point where the liver could increase the plasma protein level, the edema was relieved with high diuresis and increased cardiac output by the end of 12 days.

In figure 6 are shown the results of atrioventricular fistula simulation (4. benchmark experiment). Opening the fistula caused an immediate dramatic change in cardiac output, total peripheral resistance and heart rate. Urinary output decreased to minimal threshold levels. As the body adapted, extracellular fluid volume and blood volume increased to compensate for the fistula with the result that after a few days arterial pressure, heart rate and urinary output were near normal levels, while cardiac output doubled and peripheral resistance halved. When the fistula was closed, a dramatic effect occurred with a rapid decrease in cardiac output, rapid increase in peripheral resistance, moderate increase in arterial pressure and moderate decrease in heart rate. Marked diuresis reduced the extracellular fluid volume and blood volume to normal or slightly below. After 9 days, the patient was nearly normal.

Discussion and Conclusion

The main goal of this paper is the implementation of the core circulatory dynamics model based on Guyton's original diagram and its validation with real experimental data. It was shown how a model might furnish a physiological interpretation for the statistical results obtained on clinical data. We also used the output from Guyton experiments (Guyton *et al.* 1972) as a benchmark to validate our implementation. One such problem is the regulation of arterial blood pressure, as was well established by Guyton and his collaborators, since their

quantitative systems models led them to a deep reorientation of the understanding of the causes of hypertension (Guyton *et al*. 1967, Guyton 1980, Guyton 1990). This was our rationale for adopting Guyton diagram as the initial demonstrator of the core model.

As an example of general reflection on physiological regulation, we further discussed the significant differences between the output of the last two simulations including nephrosis and atrioventricular fistula. Both experiments are associated with significant changes in kidneys functions; involving changes in urinary output, arterial pressure, cardiac output, and plasma or blood volume. In simulation of the circulatory changes in nephrosis, the seven-fold rate of plasma-protein loss caused a fast decrease of proteins volume in the plasma. Reduced oncotic pressure of proteins led to a transfer of water from plasma into interstitium, and a decrease of plasma volume which caused a decrease in arterial pressure. The decreased volume of plasma led also to a decrease of pressure in atriums followed by a decrease of the cardiac output. As a result of decreased arterial pressure, vasoconstrictor effects of autonomic autoregulation caused a rapid decrease of urinary output. Reduced volume of plasma proteins lowered the intake of oncotic pressure of proteins in glomerular capillaries, and thus caused an increase in glomerular filtration and sequential diuresis. Continuous transfer of water from plasma into interstitium and a decrease in arterial pressure resulted in a slow decrease of diuresis into minimal threshold levels. Considering that a simulated patient could not lose more plasma proteins through the kidneys, the rate of plasma protein loss was reduced to three-fold of the norm after 7 days of the experiment. This effect was sufficient to stop the decrease and sequential increase of the concentration of plasma proteins in consequence of proteins synthesis progress in the liver. Considering water accumulation in interstitium, the interstitial fluid pressure increased, a slight increase of proteins was sufficient to invert equilibrium on the capillary membrane, and water began to resorb from interstitium to plasma. This was associated with increased plasma volume and sequential diuresis. The results from the

simulation are almost identical with those that occur in patients with nephrosis (Guyton *et al.* 1972, Lewis *et al.* 1998). This includes the failure to develop sufficient amounts of edema until the protein concentration falls below a critically low level of about third of normal (Guyton *et al.* 1972). The simulation also shows the typical tendency for nephrotic patients to have a mild degree of circulatory collapse and slightly decreased plasma volumes (Guyton *et al.* 1972). Another important effect is the changing level of urinary output, a feature that also occurs in nephrotic patients, with urinary output falling very low during those periods where large amounts of edema are being actively formed and the urinary output becoming great during those periods when edema is being resorbed (Guyton *et al.* 1972).

Simultaneously as the simulation of nephrosis, simulation of the atrioventricular fistula was associated with an initial rapid decrease of urinary output. Opening the fistula caused a dramatic decrease of peripheral resistance and an immediate increase of cardiac output. This resulted in acute reaction of autonomic system which rapidly decreased glomerular filtration using increase of resistance, and thus practically stopped the urinary output. As a consequence of the stopped urinary output, the blood volume was increased, vasoconstrictor reaction in kidneys was subsided, and diuresis was re-established. Circulatory system dynamics shifted to its new dynamic equilibrium with increased cardiac output and blood volume, and decreased peripheral resistance. After closure of the fistula, this whole process was reoriented. The kidneys rapidly urinated redundant blood volume and circulatory dynamics system returned to normal levels. The results from the simulation are almost identical with those that occur during clinical observation of the effects of closing and opening a fistula in animals (Frank *et al.* 1955). An important effect of fistula management can be found in (Friesen *et al.* 2000). This simulation among others shows the essential importance of renal blood volume control for maintenance of blood pressure.

Our circulatory dynamics model can also be used to simulate other experiments including simulations of development of general heart failure, effects of sympathetic nervous system removal on circulatory function, effect of infusion of different types of substances, effects of vasoconstrictor agents acting on different parts of the circulation, effects of extreme reduction of renal function on circulatory function, and others. Created SIMULINK diagram involves tracking the values of physiological functions during simulation experiments and also disconnect the individual regulation circuits using switches. It allows tracking the importance of individual regulation circuits in progression of a number of various pathological conditions. As an example, in atrioventricular fistula experiment, when the AUM-parameter (sympathetic arterial effect on arteries) in the kidneys is returned to its normal value, the kidneys will not respond on increased autonomic system activity. Similarly, in the nephrotic experiment, when the PPC-parameter (plasma colloid osmotic pressure) is returned to its normal value, the kidneys will not increase diuresis in response to the decrease of plasma protein volume. The restored Gyuton diagram has become an interactive educational aid that allows through model experiments, a better reflection on general physiological regulations in pathogenesis of various diseases.

The result of this study is not only a complex functional model, but also a correction of the frequently published Guyton diagram, which still remains a landmark achievement. The model evolved over the years, but the core of the model and the basic concepts remained untouched and many of the principles contained in the original model have been incorporated by others into advanced models (Abram *et al.* 2007, Hester *et al.* 2008). The originality of our core model implementation is our commitment to providing documentation for each basic module and continuous interactive modification and development of any aspect of the model parameters or equation and its documentation. The complex medicine simulator based on the quantitative physiological model will make it possible to simulate a number of pathological

conditions on a virtual patient and the effect of using an artificial organ on normal physiological function can also be simulated. These include artificial heart, artificial ventilator, dialysis, and others.

Acknowledgement

This research was supported by the research programs “Studies at the molecular and cellular levels in normal and in selected clinically relevant pathologic states” MSM 0021620806, and “Transdisciplinary Research in Biomedical Engineering” MSM 6840770012, and by the grants “e-Golem: medical learning simulator of human physiological functions as a background of e-learning teaching of critical care medicine” MSM 2C06031, „Analysis and Modelling Biological and Speech Signals” GAČR 102/08/H008, and by the Grant Agency of the Czech Technical University in Prague SGS10/180/OHK3/2T/13, and by Creative Connection Ltd.

We are obliged to R. J. White for provision of FORTRAN implementation of the original Guyton *et al*. model.

References

ABRAM SR, HODNETT BL, SUMMERS RL, COLEMAN TG, HESTER RL: Quantitative circulatory physiology: an integrative mathematical model of human physiology for medical education. *Adv. Physiol. Educ*. **31**: 202–210, 2007.

BASSINGTHWAIGHTE JB: Strategies for the Physiome Project. *Ann. Biomed. Eng.* **28**: 1043-1058, 2000.

BASSINGTHWAIGHTE J, HUNTER P, NOBLE D: The Cardiac Physiome: perspectives for the future. *Exp. Physiol.* **94**: 597-605, 2009.

BRUCE NVV, MONTANI J-P: Circulation and Fluid Volume Control. In: *Integrative Physiology in the Proteomics and Post-Genomics Age*. W. Walz (eds), Humana Press, Totowa, NJ, 2005, pp. 43-66.

CHAU NP, SAFAR ME, LONDON GM, WEISS YA: Essential Hypertension: An Approach to Clinical data by the Use of Models. *Hypertension*. **1**: 86-97, 1979.

COLEMAN TG, GUYTON AC: Hypertension caused by salt loading in the dog. III. Onset transients of cardiac output and other circulatory variables. *Circ. Res.* **25**: 152-160, 1969.

COWLEY AW, GUYTON AC: Baroreceptor reflex effects on transient and steady-state hemodynamics of salt-loading hypertension in dogs. *Circ. Res.* **36**: 536-546, 1975.

DOUGLAS BH, GUYTON AC, LANGSTON JB., BISHOP VS: Hypertension caused by salt loading. II. Fluid volume and tissue pressure changes. *Am. J. Physiol.* **207**: 669-671, 1964.

FRANK CV, WANG H-H, LAMMERANT J, MILLER R, WEGRIA R: An experimental study of the immediate hemodynamic adjustments to acute arteriovenous fistulae of various sizes. *J. Clin, Invest.* **34**: 722-731, 1955.

FRIESEN CH, HOWLETT JG, ROSS DB: Traumatic coronary artery fistula management. *Ann. Thorac. Surg*. **69**: 1973-1982, 2000.

GUYTON AC, COLEMAN TG: Long-term regulation of the circulation: interrelationships with body fluid volumes. In *Physical bases of Circulatory Transport Regulation and Exchange*, edited by E. B. Reeve and A. C. Guyton. Philadelphia, PA: Saunders, 1967, pp. 179-201.

GUYTON AC, COLEMAN TG, GRANDER HJ: Circulation: Overall Regulation. *Ann. Rev. Physiol.* **41**:13-41, 1972.

GUYTON AC, JONES CE, COLEMAN TG: Circulatory Physiology: Cardiac Output and Its Regulation. WB Saunders Company, Philadelphia, 1973, p. 486.

GUYTON AC: *Arterial Pressure and Hypertension*. Philadelphia, PA: Saunders, 1980.

GUYTON AC: The suprising kidney-fluid mechanism for pressure control—its infinite gain! *Hypertension.* **16**: 725-730, (1990).

HALL JE: The pioneering use of system analysis to study cardiac output regulation. *Am. J. Physiol. Regul. Integr. Comp. Physiol.* **287**: 1009-1001, 2004.

HESTER RL, COLEMAN T, SUMMERS R: A multilevel open source integrative model of human physiology. *The FASEB Journal*. **22**: 756.8, 2008.

HUNTER PJ, ROBINS P, NOBLE D: The IUPS Physiome Project. *Pflugers Archiv - European Journal of Physiology.* **445**: 1-9, 2002.

KOFRÁNEK J, RUSZ J: From graphic diagrams to educational models. *Cesk. Fysiol*. **56**: 69–78, 2007.

LANGSTON JB, GUYTON AC, DOUGLAS BH, DORSETT PE: Effect of changes in salt intake on arterial pressure and renal function in nephrectomized dogs. *Circ. Res.* **12**: 508-513, 1963.

LEWIS DM, TOOKE JE, BEAMAN M, GAMBLE H, SHORE AC: Peripheral microvascular parameters in the nephrotic syndrome. *Kidney Int*. **54**: 1261-1266, 1998.

MANNING RD, COLEMAN TG, GUYTON AC, NORMAN RA, McCAA RE: Essential role of mean circulatory filling pressure in salt-induced hypertension. *Am. J. Physiol*. **236**: 40-R7, 1979.

MONTANI J-P, VAN VLIET BN: Understanding the contribution of Guyton's large circulatory model to long-term control of arterial pressure. *Exp. Physiol.* **94**: 382-388, 2009.

NGUYEN CN, SIMANSKI O, KAHLER R, et al.: The benefits of using Guyton's model in a hypotensive control system. *Comput. Meth. Prog. Bio*. **89**: 153-161, 2008.

OSBORN JW, AVERINA VA, FINK GD: Current computational models do not reveal the importance of the nervous system in long-term control of arterial pressure. *Exp. Physiol.* **94**: 389-396, 2009.

SRINISAVAN RS, LEONARD JI, WHITE RJ: Mathematical modelling of physiological states. *Space biology and medicine*. **3**: 559-594, 1996.

THOMAS SR, BACONNIER P, FONTECAVE J, et al.: SAPHIR: a physiome core model of body fluid homeostasis and blood pressure regulation. *Phil. Trans. R. Soc. A*. **366**: 3175-3197, 2008.

WHITE RJ, LEONARD JI, SRINIVASAN RS, CHARLES JB: Mathematical modelling of acute and chronic cardiovascular changes during extended duration orbiter (EDO) flights. *Acta Astronaut.* **23**: 41–51, 1991.

WHITE RJ, BASSINGTHWAIGHTE JB, CHARLES JB, KUSHMERICK MJ, NEWMAN DJ: Issues of exploration: human health and wellbeing during a mission to Mars. *Adv. Space Res.* **31**: 7–16, 2003.

Table 1 List of state variables used in the original Guyton diagram with physiological significances, block numbers, and abbreviations.

State variable in selected subsystem	Block number	Abbreviation
Circulatory dynamics	**1 - 60**	-
01. Venous vascular volume	6	VVS
02. Right atrial volume	13	VRA
03. Volume in pulmonary arteries	19	VPA
04. Volume in left atrium	25	VLA
05. Volume in systemic arteries	31	VAS
Vascular stress relaxation	**61 - 65**	-
06. Increased vascular volume caused by stress relaxation	65	VV7
Capillary membrane dynamics	**66 - 82**	-
07. Plasma volume	71	VP
08. Total plasma protein	80	PRP
Tissue fluids, pressure and gel	**83 - 113**	-
09. Total interstitial fluid volume	84	VTS
10. Volume of interstitial fluid gel	101	VG
11. Interstitial fluid protein	103	IFP
12. Total protein in gel	112	GPR
Electrolytes and cell water	**114 - 135**	-
13. Total extracellular sodium	118	NAE
14. Total extracellular fluid potassium	122	KE
15. Total intracellular potassium concentration	131	KI
Pulmonary dynamics and fluids	**136 - 152**	-
16. Pulmonary free fluid volume	142	VPF
17. Total protein in pulmonary fluids	149	PPR
Angiotensin control	**153 - 163**	-
18. Angiotensin concentration	159	ANC
Aldosterone control	**164 - 174**	-
19. Aldosterone concentration	170	AMC
Antidiuretic hormone control	**175 - 189**	-
20. Degree of adaption of the right atrial pressure	180	AHY
21. Antidiuretic hormone concentration	185	AHC
Thirst and drinking	**190 - 194**	-
Kidney dynamics and excretion	**195 - 222**	-
Muscle blood flow control and PO2	**223 - 254**	-
22. Rate of increase in venous vascular volume	231	DVS
23. Total volume of oxygen in muscle cells	238	QOM
24. Muscle vascular constriction caused by local tissue control	254	AMM
Non-muscle oxygen delivery	**255 - 272**	-
25. Non-muscle venous oxygen saturation	260	OSV
26. Non-muscle total cellular oxygen	271	QO2
Non-muscle, non-renal local blood flow control	**273 - 290**	-
27. Vasoconstrictor effects of rapid autoregulation	278	AR1
28. Vasoconstrictor effects of intermediate autoregulation	285	AR2
29. Vasoconstrictor effects of long-term autoregulation	289	AR3
Autonomic control	**291 - 320**	-
30. Time delay for realization of autonomic drive	305	AU4
31. Overall activity of autonomic system	310	AUJ
Heart rate and stroke volume	**321 - 328**	-
Red cells and viscosity	**329 - 339**	-
32. Volume of red blood cells	332	VRC
33. Hematocrit	336	HM2
Hearth hypertrophy or deterioration	**329 - 352**	-
34. Hypertrophy effect on left ventricle	344	HPL
35. Hypertrophy effect on heart	349	HPR
36. Cardiac depressant effect of hypoxia	352	HMD

Figure 1 Block diagram of the original Guyton *et al.* model subscribed by subsystems.

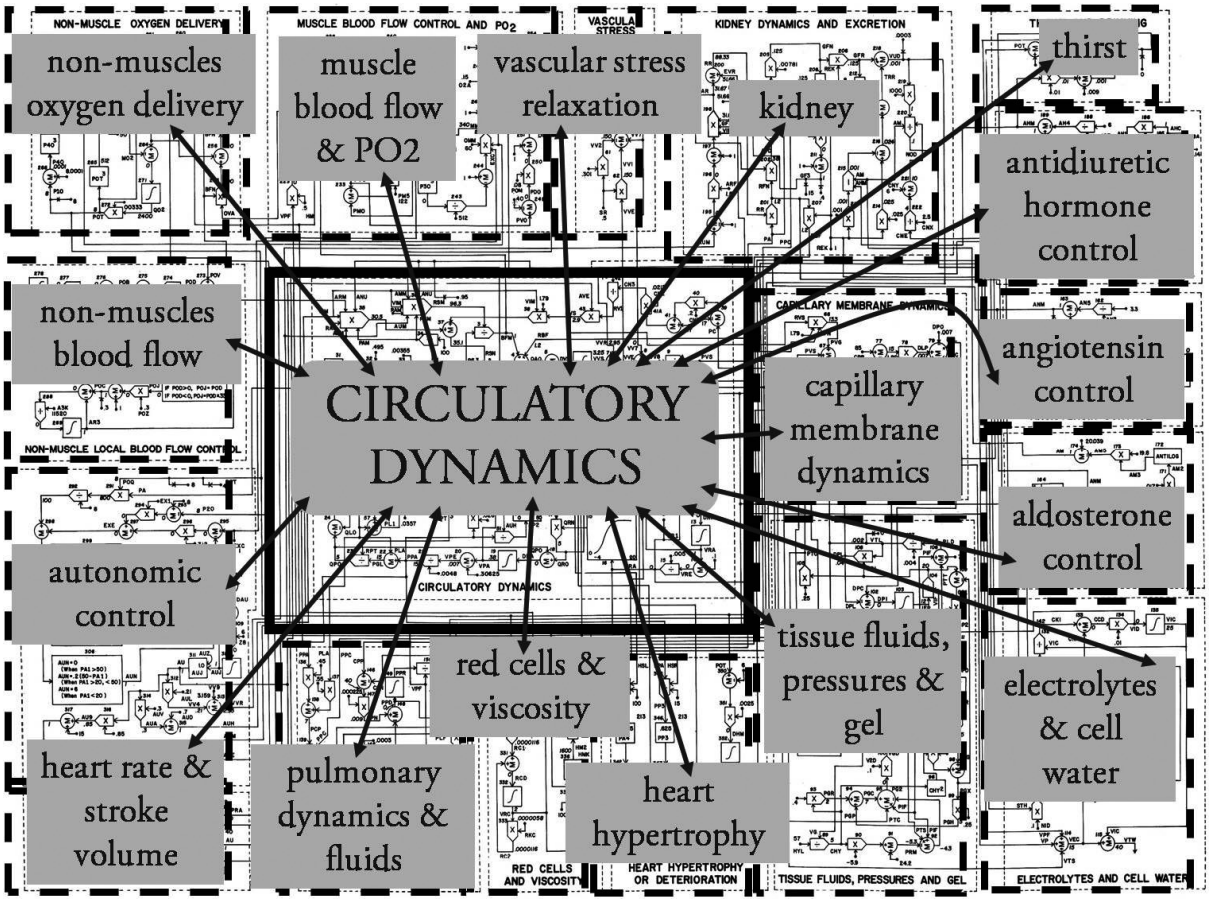

Figure 2 The most significant errors of the original diagram and their correction.

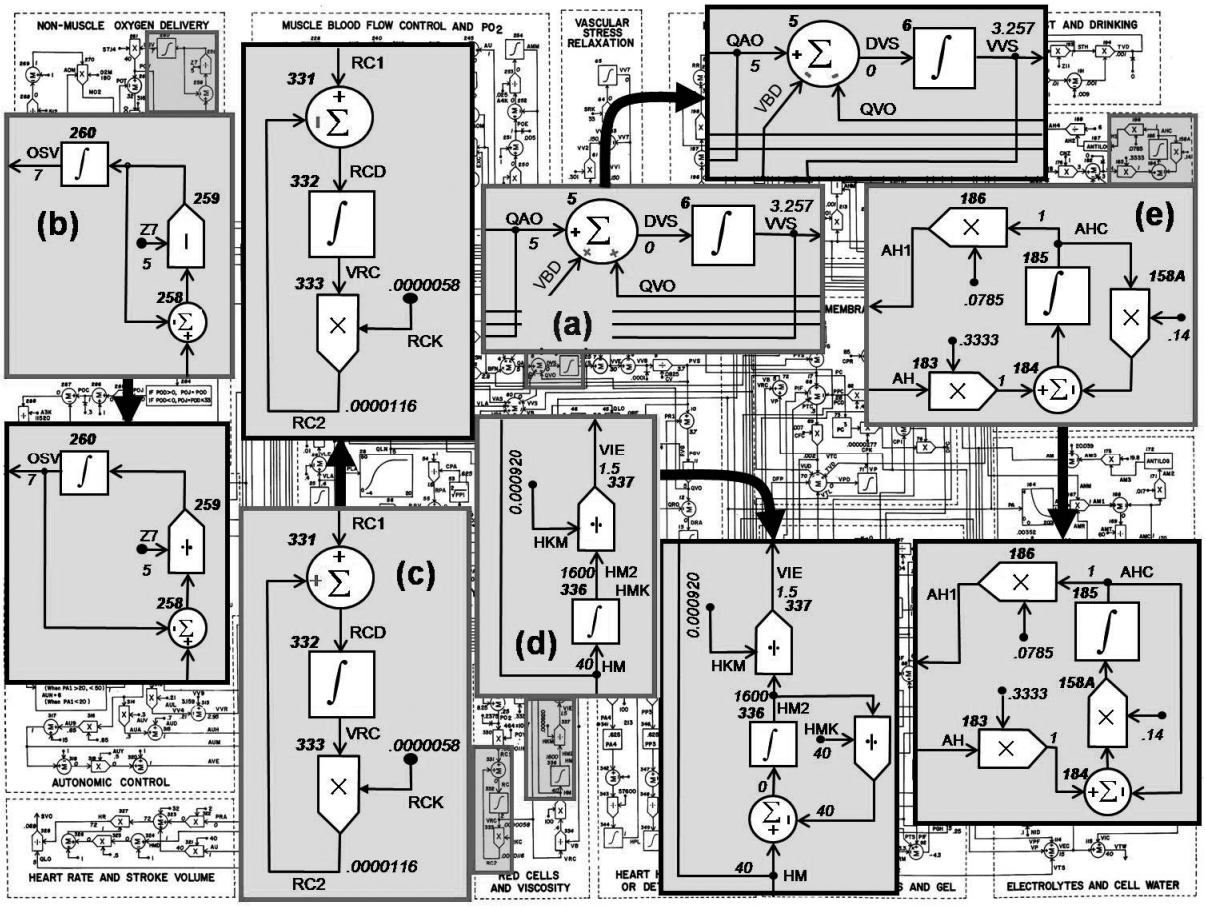

Figure 3 Simulation of changes in circulatory function at the onset of hypertension caused by reduction of renal mass and an increase in salt intake. Left: Transient changes of different variables in a series of six dogs in which 70% of the renal mass had been removed and intravenous infusion of saline at a rate of 2 to 3 liters per day was given for 12 days (data adopted from Chau *et al.* 1979). Right: Model simulation of the same experiment as that seen on the left in dogs; performed by our corrected implementation in SIMULINK (solid lines) in comparison with original 1972 Guyton *et al*. implementation in FORTRAN (dashdot lines). Changes in all variables are essentially similar to those found in the animals.

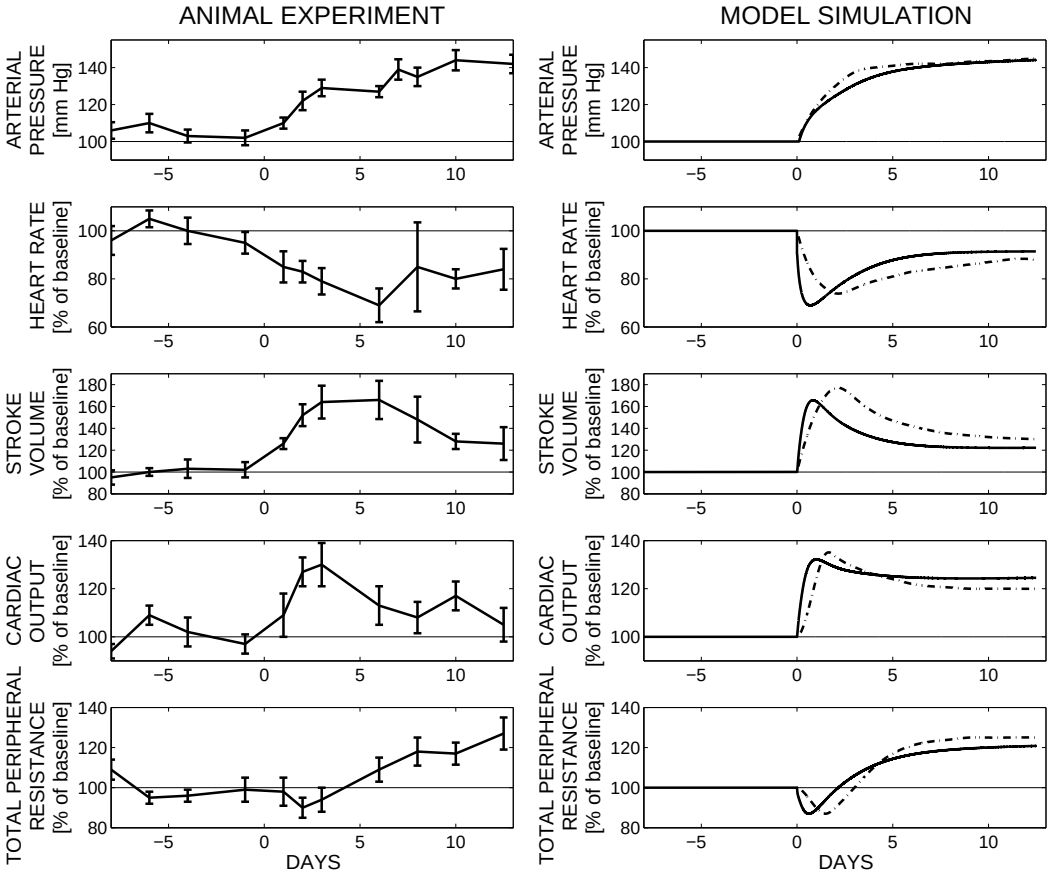

Figure 4 Benchmark experiment 2: simulation of circulatory dynamics during muscle exercise. At initial break in the curves, the muscles were activated to a level 60 times their normal value. After two minutes, the degree of activation returned to normal. Total experiment time (x -axis) was 5 minutes. Comparison of simulation results of our SIMULINK model (solid lines) with the original Guyton *et al.* model implementation in FORTRAN (dashdot lines).

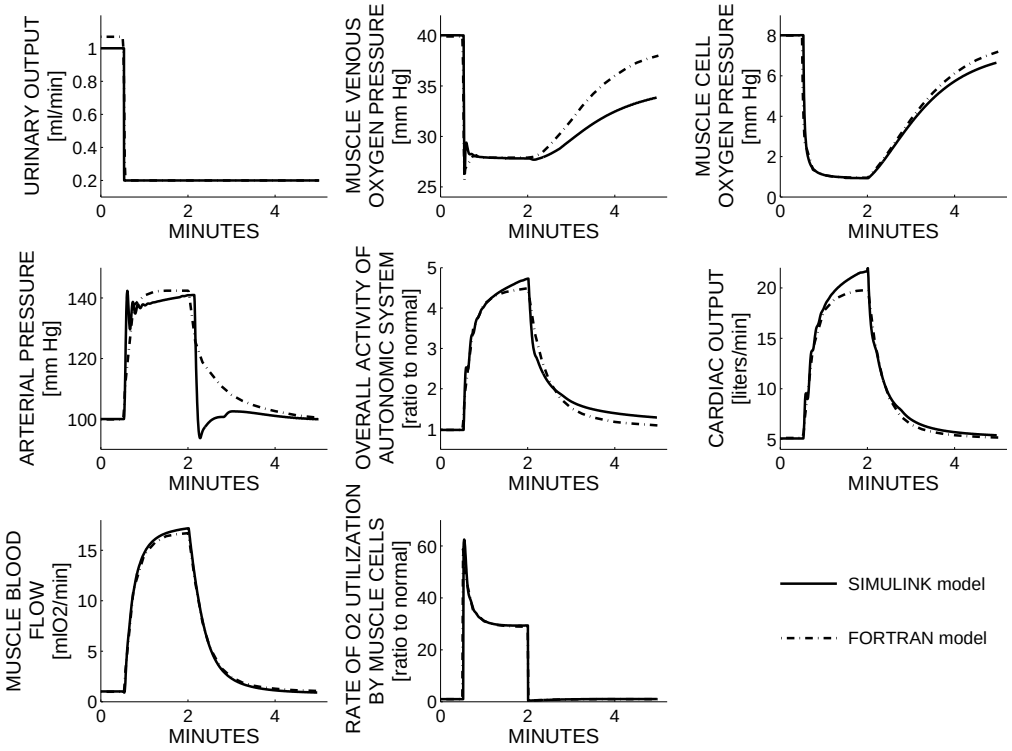

Figure 5 Benchmark experiment 3: simulation of circulatory dynamics in nephrosis. At day 1, the kidneys began to excrete large amount of plasma protein. As a consequence, the fall of the total circulating plasma protein occurred. When the plasma total protein fell below a critical level, an enormous increase in interstitial free fluid occured. At the end of simulation, an increase in total plasma protein caused marked diuresis and beginning resorption of the edema. Total experiment time (x -axis) was 288 hours (12 days). Comparison of simulation results of our SIMULINK model (solid lines) with the original Guyton *et al.* model implementation in FORTRAN (dashdot lines).

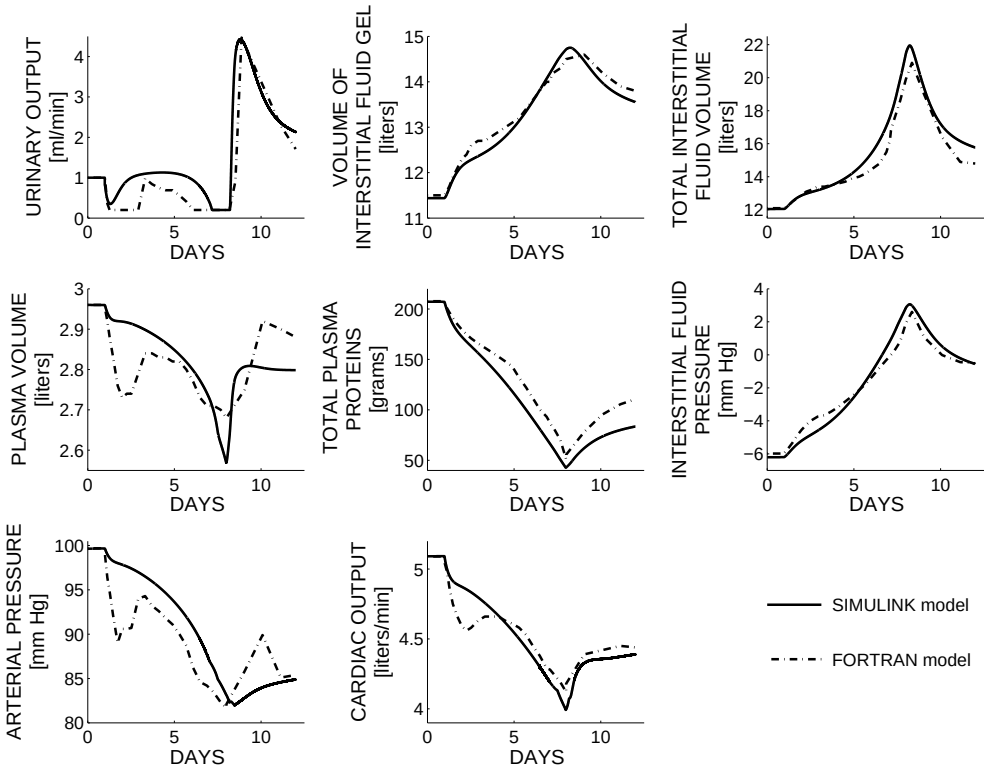

Figure 6 Benchmark experiment 4: simulation of atrioventricular fistula. At day 1, the opening of the fistula caused an extreme increase in cardiac output, and decrease in total peripheral resistance. It remains until 5 day where the fistula was closed. At the end of the record, patient was nearly normal. Total experiment time (x -axis) was 9 days. Comparison of simulation results of our SIMULINK model (solid lines) with the original Guyton *et al.* model implementation in FORTRAN (dashdot lines).